

This is the peer reviewed version of the following article: [Wejnerowski Ł., Poniecka E., Buda J., Klimaszyk P., Piasecka A., Dziuba M.K., Mugnai G., Takeuchi N., Zawierucha K. 2023. *Empirical testing of cryoconite granulation: Role of cyanobacteria in the formation of key biogenic structure darkening glaciers in polar regions*. *Journal of Phycology* 59: 939-949], which has been published in final form at [<https://doi.org/10.1111/jpy.13372>]. This article may be used for non-commercial purposes in accordance with Wiley Terms and Conditions for Use of Self-Archived Versions. This article may not be enhanced, enriched or otherwise transformed into a derivative work, without express permission from Wiley or by statutory rights under applicable legislation. Copyright notices must not be removed, obscured or modified. The article must be linked to Wiley's version of record on Wiley Online Library and any embedding, framing or otherwise making available the article or pages thereof by third parties from platforms, services and websites other than Wiley Online Library must be prohibited.

1 EMPIRICAL TESTING OF CRYOCONITE GRANULATION: ROLE OF
2 CYANOBACTERIA IN THE FORMATION OF KEY BIOGENIC STRUCTURE
3 DARKENING GLACIERS IN POLAR REGIONS

4 **Running head:** Formation of cryoconite granules

5
6 *Łukasz Wejnerowski*

7 <https://orcid.org/0000-0002-2690-4302>

8 Department of Hydrobiology, Institute of Environmental Biology, Faculty of Biology, Adam
9 Mickiewicz University, 61-614 Poznań, Poland

10
11 *Ewa Poniecka*

12 <https://orcid.org/0000-0002-0772-8630>

13 Department of Environmental Microbiology and Biotechnology, Faculty of Biology,
14 University of Warsaw, 02-096 Warsaw, Poland

15
16 *Jakub Buda*

17 <https://orcid.org/0000-0002-4584-5897>

18 Department of Animal Taxonomy and Ecology, Faculty of Biology, Adam Mickiewicz
19 University, 61-614 Poznań, Poland

20
21 *Piotr Klimaszyk*

22 <https://orcid.org/0000-0003-2847-1106>

23 Department of Water Protection, Faculty of Biology, Adam Mickiewicz University, 61-614
24 Poznań, Poland

26
27
28
29
30
31
32
33
34
35
36
37
38
39
40
41
42
43
44
45
46
47
48
49
50

Agnieszka Piasecka

<https://orcid.org/0000-0001-5686-886X>

Department of Gene Expression, Institute of Molecular Biology and Biotechnology, Faculty
of Biology, Adam Mickiewicz University, 61-614 Poznań, Poland

Marcin Krzysztof Dziuba

<https://orcid.org/0000-0003-1803-4164>

Department of Ecology and Evolutionary Biology, University of Michigan, 48109 Ann Arbor,
USA

Gianmarco Mugnai

<https://orcid.org/0000-0002-0130-7683>

Department of Agriculture, Food and Environmental Sciences, University of Perugia
Borgo XX Giugno, 74, I-06121, Perugia, Italy

Nozomu Takeuchi

<https://orcid.org/0000-0002-3267-5534>

Department of Earth Sciences, Graduate School of Science, Chiba University, 2638522
Chiba, Japan

and Krzysztof Zawierucha¹

<https://orcid.org/0000-0002-0754-1411>

Department of Animal Taxonomy and Ecology, Faculty of Biology, Adam Mickiewicz
University, 61-614 Poznań, Poland

51 ¹ Author for correspondence: Krzysztof Zawierucha (k.zawierucha@amu.edu.pl)

52 **Abstract**

53 Cryoconite, the dark sediment on the surface of glaciers, often aggregates into oval or irregular
54 granules serving as biogeochemical factories. They reduce a glacier's albedo, act as biodiversity
55 hotspots by supporting aerobic and anaerobic microbial communities, constitute one of the
56 organic matter (OM) sources on glaciers and are a feeder for micrometazoans. Although
57 cryoconite granules have multiple roles on glaciers, their formation is poorly understood.
58 Cyanobacteria are ubiquitous and abundant engineers of cryoconite hole ecosystems. This study
59 tested whether cyanobacteria may be responsible for cryoconite granulation as a sole biotic
60 element. Incubation of Greenlandic, Svalbard and Scandinavian cyanobacteria in different
61 nutrient availability and substratum for the growth (distilled water alone, and water with either
62 quartz powder, furnaceed cryoconite without OM or powdered rocks from glacial catchment)
63 revealed that cyanobacteria bind mineral particles into granules. The structures formed in the
64 experiment resembled those commonly observed in natural cryoconite holes: they contained
65 numerous cyanobacterial filaments protruding from aggregated mineral particles. Moreover, all
66 examined strains were confirmed to produce extracellular polymeric substances (EPS), which
67 suggest that cryoconite granulation is most likely due to EPS secretion by gliding cyanobacteria.
68 In the presence of water as the only substrate for growth, cyanobacteria formed mostly carpet-
69 like mats. Our data empirically prove that EPS-producing oscillatorialean cyanobacteria
70 isolated from the diverse community of cryoconite microorganisms can form granules from
71 mineral substrate and that the presence of the mineral substrate increases the probability of the
72 formation of these important and complex biogeochemical microstructures on glaciers.

73

74 **Key index words:** Alcian blue staining, biogenic aggregations, cryoconite granules,
75 extracellular polymeric substances, glacial ecosystems, glacier cyanobacteria, Oscillatoriales,
76 *Phormidesmis*, *Microcoleus*, scanning electron microscopy

77 ***Abbreviation:***

78 EPS, extracellular polymeric substances

79 OM, organic matter

80 SEM, scanning electron microscopy

81 INTRODUCTION

82 The significance of cryoconite, the dark sediment on the glacier surface, for the functioning
83 of the glacial ecosystems has been discussed in the literature for decades (Cook et al., 2015,
84 Kohshima et al., 1993, Rozwalak et al., 2022, Takeuchi et al., 2001). It substantially reduces
85 albedo of the glacier surface and speeds-up ice melting (Kohshima et al., 1993, Li et al., 2019)
86 which results in formation of cryoconite holes – freshwater ecosystems in the ice surface
87 (Fountain et al., 2004, Zawierucha et al., 2018). In some regions, sediments aggregate into
88 spherical and/or irregular forms called cryoconite granules (Rozwalak et al., 2022, Takeuchi et
89 al., 2001), which support aerobic and anaerobic microbial communities (Segawa et al., 2020).
90 They have great importance for the biogeochemical function of the glacier surface, sustaining
91 biodiversity hotspots and serving as refuges and feeders for microorganisms on glaciers (e.g.
92 Segawa et al., 2020, Zawierucha et al., 2018, Žárský et al., 2013). Such aggregates significantly
93 darken the surface of ice and trigger warming of the glacial surface (Leidman et al., 2020,
94 Takeuchi et al., 2001).

95 It has been hypothesised that cryoconite granules are formed as a result of microbial
96 activity in the cryoconite (Rozwalak et al., 2022). Fundamental papers of Takeuchi et al. (2001,
97 2010) and Langford et al. (2010, 2014) suggested that extracellular polymeric substances (EPS),
98 secreted by cyanobacteria and other EPSs producers (e.g. heterotrophic bacteria, microalgae),
99 are responsible for cryoconite granulation. EPSs are organic polymers, constituted by
100 polysaccharides, proteins, nucleic acids, and amphiphilic substances such as (phospho)-lipids
101 (Wingender et al., 1999). The role of the microbial EPS is crucial in many ecosystems from the
102 biological soil crust (soil ecosystem) to algal blooms (aquatic ecosystem) (Liu et al., 2018,
103 Rossi et al., 2018). The excretion of EPSs is an important physiological process that promotes
104 cell adhesion and cohesion, improves the resilience to freezing and thawing, helps the
105 accumulation of minerals and nutrients and also protects the microorganisms from UV-

106 radiation (Rossi et al., 2018). Moreover, due to great cohesive properties, the aggregation of
107 organisms and minerals acts as a refuge against consumers (like protozoan predation). In
108 addition, organisms in symbiotic aggregates can benefit through the mutual use of nutrients, as
109 shown in the example of cryoconite granules, where heterotrophic bacteria use compounds
110 produced by cyanobacteria, while cyanobacteria can use those produced by heterotrophic
111 bacteria inside the granules (Segawa et al., 2020). Therefore, the role of EPSs seems to be
112 crucial for the biogeochemistry of cryospheric habitats (Nagar et al., 2021, Segawa et al., 2020,
113 Takechi et al., 2001). Hence, it has been suggested that cyanobacteria abundant on glaciers are
114 a substantial element shaping the structure of cryoconite (Rozwalak et al., 2022, Takeuchi et
115 al., 2010). Despite the crucial, multilevel role of cryoconite granules, experimental studies on
116 cryoconite granulation are surprisingly scarce. A laboratory experiment conducted by Musilova
117 et al. (2016) showed the great importance of light and nutrients to cryoconite granule formation
118 by the microbial community. In turn, Langford (2012) revealed that lake isolates of Antarctic
119 filamentous cyanobacteria (*Leptolyngbya* cf. *antarctica*, *Wilmottia murrayi*) can use mineral
120 grains to form granules when a nutrient-rich liquid medium is applied.

121 In this study, we tested whether Arctic filamentous cyanobacteria isolated directly from
122 cryoconite sediments can granulate cryoconite under poor nutrient levels and at low
123 temperatures – the environment that reflects semi-natural conditions in the cryoconite hole. In
124 our empirical test on cryoconite granulation, several oscillatoriallean cyanobacteria isolates
125 were inoculated into the plastic wells filled with distilled water and different types of mineral
126 substrates. Using powdered form of substrates, we reflected the transfer of tiny mineral
127 substrates by wind to the glacier surface, thereby we were able to track cryoconite granulation
128 phenomenon from the starting point. During several months of incubation, cultures were
129 monitored for physical structure formation. We also checked if our model cyanobacterial strains

130 are able to produce EPSs, which is recognized as a main factor triggering the microbial
131 aggregation and cryoconite granulation.

132

133

134 METHODS

135 *Cyanobacteria strains and culturing technique.* Cyanobacteria were obtained from cryoconite
136 collected from four localities in the Arctic: Longyearbreen Glacier in Svalbard (78° 10' N, 15°
137 31' E), Russel Glacier (67° 9' N, 50° 0' W) and Dark Zone (67° 04' N, 49° 23' W) in South-West
138 Greenland, and Storglaciären Glacier (67° 54' N, 18°34'E) in Sweden. Samples were collected
139 with pipettes to Whirl-Pak bags or falcon tubes and then frozen and transported to the laboratory
140 and stored at -20°C. The plastic bags and falcon tubes were sterile and have not been opened
141 during the transport or in the field in order to avoid contamination. Single filaments (without
142 any attached microalgae) were isolated from cryoconite using a serial dilution technique with
143 microcapillaries (Andersen & Kawachi, 2005). As cryoconites contain various algae species
144 and heterotrophs (Perini et al., 2022, Poniecka et al., 2020, Zawierucha et al., 2018), we used
145 precise technique for isolation and culturing solely cyanobacteria. Before the isolation of
146 cyanobacterial filaments, cryoconite material was vortexed to separate cyanobacteria from
147 mineral granules. Then, single filaments were rinsed several times in imipenem antibiotic
148 solution (10 µg mL⁻¹) to remove potential bacterial contaminations (Ferris & Hirsch, 1991).
149 When an isolate was found to be contaminated with bacteria, re-isolation of filaments was
150 conducted. Purity of the cultures was assessed in dense cultures using an inverted phase contrast
151 microscope Leica DM IL LED (Leica Microsystems, Wetzlar, Germany). When microscopy
152 inspections of the cultures showed a lack of spherical, rod-shaped, curved objects or biofilms,
153 they were recognized as pure. Stock isolates were grown in well plates with wells filled with 2
154 mL of WC medium (Guillard and Lorenzen 1972). Cultures were stored in a walk-in incubator

155 under defined temperature (3°C) and light intensity (33-44 $\mu\text{mol photons m}^{-2} \text{s}^{-1}$). After about
156 seven months, we had four pure, viable and successfully growing isolates. Taxonomic
157 identification of strains was based on a combination of molecular marker (16S rRNA gene
158 sequencing; for methods of DNA extraction, amplification and phylogeny see supporting
159 information (Appendix 1)) and microscopic observations of filaments and diagnosis of their
160 key morphological features according to Komárek & Anagnostidis (2005), Teneva et al. (2023),
161 Strunecký et al. (2011), Strunecký et al. (2013).

162

163 *Experimental design.* Inocula of each strain (10 filaments per a single inoculum) were
164 transferred into the wells of 24-well plates containing either 1 mL of distilled water alone
165 (control treatment) or different types of mineral particles with 1 mL of distilled water: 1)
166 cryoconite from each sampled glacier (sterilised in 550°C to remove organic matter [OM]), 2)
167 quartz powder (\emptyset : mean = 7.38 μm , SD = 4.75 μm). Greenlandic strains were additionally
168 incubated with 3) 1 ml of distilled water and ground-up rocks (\emptyset : mean = 4.27 μm , SD = 2.58
169 μm) – a local type of minerals occurring nearby the Russell Glacier catchment. The rocks were
170 collected during the Greenlandic expeditions, and we decided to use these rocks as a potential
171 substrate for cyanobacterial growth. Mineral dust is delivered to the ice surface from local
172 Greenlandic sources (Nagatsuka et al., 2016), thus this material is an analogue to other minerals
173 wind-blown on the ice surface. Each experimental group was replicated four times. Minerals
174 were distributed in wells to cover the whole bottom and form a thin layer. Plates contained only
175 distilled water and various substrata mimicking poor nutritional conditions on the glacier
176 surface. Quartz powder contains only silica (SiO_2), rocks from Greenland were composed of
177 gneiss and granitoids. Finally, furnaceed cryoconite from each investigated glacier contained
178 original mineral substratum present on the glacier during sampling.

179 Apart from single-strain experimental cultures on various mineral substrates, we also
180 distinguished an additional group – a mixture of two Greenlandic strains – designed to test
181 whether the competition between cyanobacteria influences the rate of granule formation. The
182 detailed experimental setup is presented in Fig. 1. All cultures were incubated for 6 months
183 under the same temperature and light intensity as the ones that the stock cultures were
184 maintained in. Cyanobacterial growth was detectable microscopically after three months of
185 incubation. During the further incubation period, well plates were gently shaken at least once
186 per week to mimic natural water flow disturbance on Arctic glaciers. The time-lapse imaging
187 using microscope OLYMPUS SZ and QuickPHOTO Camera 3.0 software was conducted every
188 week for the next three months until the end of the experiment. During the microscopic imaging,
189 the formation of mats, granules and their behaviour (transition from mats to granules) were
190 noted. Regular or irregular spherical or oval shaped structures were classified as granules. In
191 turn, the thick “carpet-like” structures were identified as mats.

192

193 *Cyanobacterial EPS staining procedure.* Cyanobacterial trichomes were stained with Alcian
194 Blue dye, which is commonly used for detection of polysaccharides in cyanobacteria (e.g. Perez
195 et al., 2018, Sohm et al., 2011). The 2 mL culture volume of each strain were collected in
196 Eppendorf tubes and centrifuged for 5 min at 15 000 rpm (Rotina 380R centrifuge, Hettich,
197 Germany). Subsequently, the supernatant was removed, and the pellet was diluted with 1 mL
198 of distilled water and re-suspended in a water column by 2 min vortex-shaking. After that, 0.5
199 mL of the Alcian Blue solution (1% in H₂O, w/v) was added to the tubes. After 15 min
200 incubation, cyanobacterial biomass was centrifuged and rinsed three times with distilled water.
201 Cyanobacterial trichomes were then observed under the inverted microscope Leica DM IL LED
202 (Leica Microsystems, Wetzlar, Germany) equipped with a digital camera Jenoptik Gryphax
203 NAOS (Jenoptik Optical Systems, Jena, Germany).

204

205 *Statistical analysis.* The difference in the probability of mats and granules formations between
206 treatments was tested with binomial Generalized Linear Mixed Models with the logit link
207 function. Models tested the difference in probability of granules formation between substrates
208 (separately for granules and mats formation models) with a cyanobacterial strain as a random
209 intercept effect. The impact of the number of strains per well (one or two) on the probability of
210 granules and mat formation was tested with the substratum included as a random intercept
211 effect. The models were implemented with *glmmTMB* packaged (v1.0.2.1; Brooks et al. 2017)
212 in R 3.6.3 software (R Core Team 2020). To assess whether the implemented models have
213 significantly better goodness of fit than the null model, we compared them separately with a
214 respective null model using the Chi-square test. The R script and the data are available in
215 supporting information (Appendix 2).

216

217 RESULTS AND DISCUSSION

218 In total, we isolated four monoclonal cyanobacterial strains from four glaciers in the Arctic. All
219 of them represent Oscillatoriales (supporting information, Figure S1, Appendix 3). Three
220 strains were identified with a DNA analysis as *Phormidesmis priestleyi* (strain 101,
221 Storglaciären Glacier, Sweden, GenBank accession number OR120247; strain 102, Dark Zone,
222 South West Greenland, GenBank accession number OR120248; strain 103, Russel Glacier,
223 South West Greenland, GenBank accession number OR120249). Key morphological features
224 of our *Ph. priestleyi* strains are as follows: mats of brownish, greenish or yellowish colour;
225 filaments occurring solitarily and in irregular aggregations; filaments straight and pliant with
226 visible fine sheaths; cells inside the trichomes appear barrel-shaped, their width is less than their
227 length, ranging from 2.5 – 3.1 μm (strain 101), 2.6 – 3.9 μm (strain 102), 2.3 – 3.5 μm (strain
228 103); terminal cells with rounded end without calyptra (Fig. 2, left panel). These features match

229 the characteristics of *Ph. priestleyi* (Komárek et al., 2009). The next strain (104, Longyearbreen,
230 Spitsbergen, Svalbard, GenBank accession number OR120250) was identified with DNA
231 analysis as *Microcoleus autumnalis*). Microscopic observations revealed that filaments of this
232 strain are usually straight, rarely slightly curved (only in the case of long pieces), occurring
233 solitarily or weakly aggregated/entangled with each other, and enclosed with fine or distinct
234 sheaths. Strain 104's cell width is usually larger than its length, ranging from 5.0 to 8.1 μm . Its
235 apical cells are sometimes slightly elongated and rounded at the end. The calyptra is weakly
236 expressed. During microscopic inspection of fresh and old cultures, we did not find multiple
237 trichomes in a common sheath – the feature characteristic for *Microcoleus vaginatus* (Strunecký
238 et al., 2013), but not obligatorily present in strains (Teneva et al., 2023). Taxonomic revision
239 of the genus *Microcoleus* is needed, especially given the high diversity and wide distribution
240 of strains and the existence of numerous lineages in which new species could be present
241 (Stanojković et al., 2022).

242 Both *Ph. priestleyi* and *M. autumnalis* have been earlier reported from the cryosphere
243 (Christmas et al., 2015, 2016, Strunecký et al., 2010, 2013) and can produce EPS (Christmas et
244 al., 2015, 2016, Mugnai et al., 2018, Pajdak-Stós et al., 2001, Vicente Garcia et al., 2004).
245 Alcian blue staining of cyanobacterial filaments from examined strains confirmed the presence
246 of sheaths surrounding the filaments in all strains. The sheath of *Phormidesmis priestleyi* strain
247 101 (Fig. 2A) was closed at the ends and visible only when empty, while in the *Ph. priestleyi*
248 strain 102 (Fig. 2B), the non-lamellar sheath was strictly adherent to the trichomes. In the *Ph.*
249 *priestleyi* strain 103, the sheath is wavy and sometimes lamellar (Fig. 2C). *Microcoleus*
250 *autumnalis* strain 104 is characterized by a well-defined sheath (Fig. 2D). In case of strains 102,
251 103 and 104, observation of trichomes stained with Alcian Blue revealed the presence of slime
252 outside the sheath. As we can clearly see in Fig. 2B, the deposition of the slime can differ along
253 the trichome.

254 Mats were formed by cyanobacteria at a similar rate when incubated in water alone or with
255 the addition of a substratum (sterilised cryoconite – OM free, quartz powder or grinded rocks,
256 the latter two representing silt fraction), with no difference between substrate types (Fig. 3A; χ^2
257 = 2.247, $df = 3$, $p = 0.523$). However, the probability of granule formation was significantly
258 higher in water with some substratum than without it (Fig. 3B; $\chi^2 = 6.603$, $df = 2$, $p = 0.037$); no
259 differences were found between substrate types. The formation of artificial granules from
260 North-West Greenland is shown in Fig. 4. Mats and other artificial granules are presented in
261 supporting information (Appendix 4). There was no difference in the probability of granules or
262 mats formation between groups with one or two mixed strains (granules: $\chi^2 = 0.591$, $df = 1$, $p =$
263 0.442 ; mats: $\chi^2 = 0.057$, $df = 1$, $p = 0.811$).

264 We observed that the surface of granules was usually overgrown by cyanobacteria
265 filaments (Fig. 5). Their presence in and on granules was also visible on SEM photos: particles
266 in the granules were stuck together, though in some cases we documented cyanobacterial
267 filaments protruding beyond the cryoconite granules. These filaments were often attached to
268 the bottom of the SEM stub of the sample as well. The SEM images confirmed the presence of
269 the EPS slime surrounding the filaments produced by *M. autumnalis* strain 104 (Fig 6A). *Ph.*
270 *priestleyi* strain 102 (Fig. 6B) showed filament bundles that appeared as a blanket over the
271 surface of granules, which had porous structure and interspaces. In the SEM picture of *Ph.*
272 *priestleyi* strains 102 and 103, the cyanobacterial extracellular secretion acts as a gluing agent,
273 forming organic bridges and binding filaments together (Fig. 6C). Such structures like EPS
274 bridges have earlier been found by Román et al. (2021) in crusts formed by EPSs of soil
275 cyanobacterium *Nostoc commune*.

276 Recently, Rozwalak et al. (2022) as well as Park & Takeuchi (2021) discussed potential
277 factors controlling the formation of cryoconite granules. The main hypothesised factor was the
278 presence of cyanobacteria with the ability to secrete EPS with a different level of gelification.

279 Here, we provide the first evidence that the formation of cryoconite granules on simulated
280 glacier surface conditions (cyanobacteria kept with minerals in distilled water at a low
281 temperature) is driven by the presence of cryoconite cyanobacteria strains that produce EPS.
282 Their proliferation and activity (gliding on mineral particles or squeezing between them) result
283 in binding fine mineral particles into larger and larger granules. Direct evidence on extracellular
284 polymeric substances (EPSs) produced by the examined strains corroborates the hypothesis that
285 cryoconite granulation phenomenon is due to the cyanobacterial EPS that promote the mineral
286 grains aggregation. Although we have observed few spherical structures in treatments without
287 substratum in strain 101 from Storglaciären Glacier, they did not form cemented structures but
288 rather consortia of integrated cyanobacteria filaments. At the same time, the richness of
289 nutrients originating from grain material (grinded rocks from glacial catchment, cryoconite
290 sterilised at 550°C, quartz powder) does not influence the probability of granules formation.
291 These results suggest that glacier cyanobacteria are highly resilient to extremely low nutrient
292 content, and grow in both water and water mixed with mineral particles. Nevertheless, we
293 cannot exclude some minor transfer of nutrients during inoculation of cyanobacterial filaments
294 from stock cultures into the wells at the beginning of the experiment, as WC medium (that stock
295 cultures were reared in) is rich in nutrients. However, for the inoculation of cyanobacteria, we
296 used very fine microcapillaries of ~10 µm diameter, minimising the amount of medium
297 transferred into the wells. Hence, the enrichment of experimental wells with extra nutrients was
298 at most negligible.

299 The presence of the substrate is positively related to granules formation. Rozwalak et al.
300 (2022) found that cryoconite granules are more frequent on glaciers in the northern hemisphere
301 and are less common in the southern hemisphere, even though cyanobacteria in Antarctica
302 produce EPS. The results of our study indicate that these differences may stem, at least in part,
303 from the fact that cryoconite holes investigated by authors in the southern hemisphere consisted

304 of gravel fraction rather than silt (Rozwalak et al., 2022); that may impede formation of
305 granules. Fine mineral particles are usually lighter, thereby they can be transported with gliding
306 cyanobacterial filaments, probably until their mass does not exceed critical gliding capability
307 of a given cyanobacterial filament. The stickiness of cyanobacterial EPS is more suitable for
308 fine mineral particles aggregations. Therefore, small minerals may also perform the role of a
309 scaffold for cyanobacteria. Additionally, in a nutrient-poor environment, cyanobacteria can
310 start biological weathering (Zawierucha et al., 2019). For example, the attachment of cells to
311 the mineral surface is an important factor in microbial-mediated dissolution of rocks in glacial
312 forefield (Frey et al., 2010). As was shown by Uetake et al. (2016), there is a strong correlation
313 between mineral and cyanobacteria abundance on glaciers. The silt and sand mineral supply on
314 glaciers is, therefore, a fundamental factor for cyanobacterial growth and consequently for
315 cryoconite granules formation as was proved here experimentally. Neither other algae species
316 nor grazing of animals on glaciers is required for the formation of granules (Langford, 2012,
317 this study); however, we cannot exclude that the presence of other microorganisms may boost
318 cryoconite granulation. Although non-EPS producing benthic cyanobacteria are rather rare in
319 polar ecosystems, their role in potential control over the ecosystem should also be identified.

320

321 CONCLUSIONS

322 The results of our study are the first evidence that EPS-producing oscillatoriacean cyanobacteria
323 as a single biotic element are responsible for cryoconite granulation phenomenon that occurs
324 commonly in cryoconite holes on glaciers. The presence of sheath and EPS slime in the
325 examined cyanobacterial strains and SEM documentation of mineral particles bonded with
326 cyanobacterial trichomes and EPS, indicate that the ability of cryoconite microorganisms to
327 produce EPS is most likely a key factor in the cryoconite granules formation. Future studies

328 should focus on the quantification of different EPS fractions (sheath and slime) to further
329 expand our knowledge on the role of EPSs in cryoconite granules formation.

330

331 ACKNOWLEDGMENTS

332 Authors are grateful to Piotr Rozwalak for his help in documenting the process of granulation.

333 Analysis of photoautotrophs in cryoconite on Longyearbreen and its relation to invertebrates

334 has been conducted within the OPUS NCN 2018/31/B/NZ8/00198 grant to K.Z. Two isolates

335 of cyanobacteria were obtained within the Bekker project (no. PPN/BEK/2020/1/00241) from

336 the Polish National Agency for Academic Exchange (NAWA) by Ł.W. Molecular analyses of

337 cyanobacterial strains and EPS straining were conducted within the project from National

338 Science Centre in Poland (project no. 2020/39/D/NZ8/02436 to Ł.W.).

339

340 AUTHOR CONTRIBUTIONS

341 ŁW, EP and KZ - conceptualisation, EP, KZ - collection of material, ŁW, EP - culturing of

342 cyanobacteria, ŁW – staining of cyanobacterial EPS and visualization. ŁW, JB, PK, KZ -

343 laboratory experiments, analysis and visualisation. AP – performing molecular analysis. MKD

344 – performing phylogenetic analyses. ŁW, KZ - writing draft of manuscript, ŁW, JB, PK, NT,

345 AP, MKD, GM, and KZ - wrote, corrected and approved final version.

346

347 COMPETING INTERESTS

348 The authors have no relevant financial or non-financial interests to disclose.

349

350 DATA AVAILABILITY STATEMENT

351 All data generated during and/or analysed during the current study are available in the

352 manuscript and supplementary materials.

353

354 REFERENCES

- 355 Andersen, R.A., & Kawachi, M. (2005). Traditional microalgae isolation techniques. *In*
356 Andersen, R.A. [Ed.] *Algal Culturing Techniques, first ed.* Elsevier Academic Press,
357 London, UK, pp. 83–100.
- 358 Brooks, M. E., Kristensen, K., van Benthem, K. J., Magnusson, A., Berg, C. W., Nielsen, A.,
359 Skaug, H. J., Maechler, M., & Bolker, B. M. (2017). glmmTMB Balances Speed and
360 Flexibility Among Packages for Zero-inflated Generalized Linear Mixed Modeling.
361 *The R Journal* 9, 378–400.
- 362 Christmas, N. A. M., Anesio, A. M. & Sánchez-Baracaldo, P. (2015). Multiple adaptations to
363 polar and alpine environments within cyanobacteria: a phylogenomic and Bayesian
364 approach. *Frontiers in Microbiology*, 6, 1070.
365 <https://doi.org/10.3389/fmicb.2015.01070>
- 366 Christmas, N. A. M., Barker, G., Anesio, A. M. & Sánchez-Baracaldo, P. (2016). Genomic
367 mechanisms for cold tolerance and production of exopolysaccharides in the Arctic
368 cyanobacterium *Phormidesmis priestleyi* BC1401. *BMC Genomics*, 17, 533.
369 <https://doi.org/10.1186/s12864-016-2846-4>
- 370 Cook, J., Edwards, A., Takeuchi, N. & Irvine-Fynn, T. (2016). Cryoconite: The dark
371 biological secret of the cryosphere. *Progress in Physical Geography*, 40, 66–111.
372 <https://doi.org/10.1177/0309133315616574>
- 373 Ferris, M. J. & Hirsch, S. F. (1991). Method for isolation and purification of cyanobacteria.
374 *Applied and Environmental Microbiology Journal*, 57, 1448–1452.
375 <https://doi.org/10.1128/AEM.57.5.1448-1452.1991>
- 376 Fountain, A. G., Tranter, M., Nysten, T. H., Lewis, K. J. & Mueller, D. R. (2004). Evolution of
377 cryoconite holes and their contribution to meltwater runoff from glaciers in the

378 McMurdo Dry Valleys, Antarctica. *Journal of Glaciology*, 50, 35–45.
379 <https://doi.org/10.3189/172756504781830312>

380 Frey, B., Rieder, S. R., Brunner, I., Plötze, M., Koetzsch, S., Lapanje, A., Brandl, H. &
381 Furrer, G. (2010). Weathering-associated bacteria from the Damma Glacier Forefield:
382 physiological capabilities and impact on granite dissolution. *Applied and*
383 *Environmental Microbiology Journal*, 76, 4788–4796.
384 <https://doi.org/10.1128/AEM.00657-10>

385 Guillard, R. R. L., & Lorenzen, C. J. (1972). Yellow-green algae with chlorophyllide c.
386 *Journal of Phycology*, 8, 10–14. <https://doi.org/10.1111/j.1529-8817.1972.tb03995.x>

387 Kohshima, S., Seko, K. & Yoshimura, Y. (1993). Biotic Acceleration of Glacier Melting in
388 Yala Glacier 9 Langtang Region, Nepal Himalaya. *Snow and Glacier Hydrology,*
389 *Proceedings of Kathmandu Symposium, IAHS Publication*, 218, 309–316.

390 Komárek, J. & Anagnostidis, K. (2005). Cyanoprocaryota. 2. Teil: Oscillatoriales. In: Büdel
391 B, Krienitz L, Gärtner G, Schagerl M (Eds.) Süßwasserflora von Mitteleuropa 19/2.
392 Elsevier GmbH.

393 Komárek, J., Kaštovský, J., Ventura, S., Turicchia, S. & Šmarda, J. (2009). The
394 cyanobacterial genus *Phormidesmis*. *Algological studies*, 129, 41–59.
395 <https://doi.org/10.1127/1864-1318/2009/0129-0041>

396 Langford, H. 2012. The microstructure, biogeochemistry and aggregation of Arctic cryoconite
397 granules, Ph.D. dissertation, University of Sheffield, Sheffield.

398 Langford, H., Hodson, A., Banwart, S. & Bøggild, C. (2010). The microstructure and
399 biogeochemistry of Arctic cryoconite granules. *Annals of Glaciology*, 51, 87–94.
400 <https://doi.org/10.3189/172756411795932083>

401 Langford, H. J., Irvine-Fynn, T. D. L., Edwards, A., Banwart, S. A. & Hodson, A. J. (2014).
402 A spatial investigation of the environmental controls over cryoconite aggregation on

403 Longyearbreen glacier. Svalbard. *Biogeosciences*, *11*, 5365–5380.
404 <https://doi.org/10.5194/bg-11-5365-2014>

405 Leidman, S. Z., Rennermalm, Å. K., Muthyala, R., Guo, Q. & Overeem, I. (2020). The presence
406 and widespread distribution of dark sediment in Greenland Ice Sheet supraglacial
407 streams implies substantial impact of microbial communities on sediment deposition
408 and albedo. *Geophysical Research Letters*, *48*, 2020GL088444.
409 <https://doi.org/10.1029/2020GL088444>

410 Li, Y., Kang, S., Yan, F., Chen, J., Wang, K., Paudyal, R., Liu, J., Qin, X. & Sillanpää, M.
411 (2019). Cryoconite on a glacier on the north-eastern Tibetan plateau: light-absorbing
412 impurities, albedo and enhanced melting. *Journal of Glaciology*, *65*, 633–644.
413 <https://doi.org/10.1017/jog.2019.41>

414 Liu, L., Huang, Q. & Qin, B. (2018). Characteristics and roles of *Microcystis* extracellular
415 polymeric substances (EPS) in cyanobacterial blooms: a short review. *Journal of*
416 *Freshwater Ecology*, *33*, 183–193. <https://doi.org/10.1080/02705060.2017.1391722>

417 Mugnai, G., Rossi, F., Felde, V. J. M. N. L., Colesie, C., Büdel, B., Peth, S., Kaplan, A. &
418 Philippis, R. D. (2018). The potential of the cyanobacterium *Leptolyngbya ohadii* as
419 inoculum for stabilizing bare sandy substrates. *Soil Biology and Biochemistry*, *127*,
420 318–328. <https://doi.org/10.1016/j.soilbio.2018.08.007>

421 Musilova, M., Tranter, M., Bamber, J. L., Takeuchi, N., & Anesio, A. M. (2016). Experimental
422 evidence that microbial activity lowers the albedo of glaciers. *Geochemical Perspectives*
423 *Letters*, *2*, 106–116. https://doi.org/10.7185/geoch_emlet.1611

424 Nagar, S., Antony, R. & Thamban, M. (2021). Extracellular polymeric substances in Antarctic
425 environments: a review of their ecological roles and impact on glacier biogeochemical
426 cycles. *Polar Science*, *30*, 100686. <https://doi.org/10.1016/j.polar.2021.100686>

427 Nagatsuka, N., Takeuchi, N., Uetake, J., Shimada, R., Onuma, Y., Tanaka, S. & Nakano, T.
428 (2016). Variations in Sr and Nd isotopic ratios of mineral particles in cryoconite in
429 Western Greenland. *Frontiers in Earth Sciences*, 4.
430 <https://doi.org/10.3389/feart.2016.00093>

431 Pajdak-Stós, A., Fiałkowska, E. & Fyda, J. (2001). *Phormidium autumnale* (Cyanobacteria)
432 defense against three ciliate grazer species. *Aquatic Microbial Ecology*, 23, 237–244.
433 <https://doi.org/10.3354/ame023237>

434 Park, C. & Takeuchi, N. (2021). Unmasking photogranulation in decreasing glacial albedo
435 and net autotrophic wastewater treatment. *Environmental Microbiology*, 23, 6391–
436 6404. <https://doi.org/10.1111/1462-2920.15780>

437 Perez, R., Wörmer, L., Sass, P. & Maldener, I. (2018). A highly asynchronous developmental
438 program triggered during germination of dormant akinetes of filamentous diazotrophic
439 cyanobacteria. *FEMS Microbial Ecology*, 94, fix131.
440 <https://doi.org/10.1093/femsec/fix131>

441 Perini, L., Gostinčar, C., Likar, M., Frisvad, J. C., Kostanjšek, R., Nicholes, M., ... & Gunde-
442 Cimerman, N. (2022). Interactions of fungi and algae from the Greenland ice
443 sheet. *Microbial Ecology*, 1–15. <https://doi.org/10.1007/s00248-022-02033-5>

444 Poniecka, E. A., Bagshaw, E. A., Sass, H., Segar, A., Webster, G., Williamson, C., ... & Tranter,
445 M. (2020). Physiological capabilities of cryoconite hole microorganisms. *Frontiers in*
446 *Microbiology*, 11, 1783.

447 R Core Team (2020). R: A language and environment for statistical computing. R Foundation
448 for Statistical Computing, Vienna, Austria. <https://www.R-project.org/>

449 Román, J.R., Roncero-Ramos, B., Rodríguez-Caballero, E., Chamizo, S. & Cantón, Y.
450 (2021). Effect of water availability on induced cyanobacterial biocrust development.
451 *Catena*, 197, 104988. <https://doi.org/10.1016/j.catena.2020.104988>

452 Rossi, F., Mugnai, G. & De Philippis, R. (2018). Complex role of the polymeric matrix in
453 biological soil crusts. *Plant Soil* 429, 19–34. [https://doi.org/10.1007/s11104-017-3441-](https://doi.org/10.1007/s11104-017-3441-4)
454 4

455 Rozwalak, P., Podkowa, P., Buda, J., Niedzielski, P., Kawecki, S., Ambrosini, R., Azzoni, R.
456 S., Baccolo, G., Ceballos, J. L., Cook, J., Di Mauro, B., Ficetola, G. F., Franzetti, A.,
457 Ignatiuk, D., Klimaszyk, P., Łokas, E., Ono, M., Parnikoza, I., Pietryka, M., Pittino,
458 F., Poniecka, E., Porazinska, D. L., Richter, D., Schmidt, S. K., Sommers, P., Souza-
459 Kasprzyk, J., Stibal, M., Szczuciński, W., Uetake, J., Wejnerowski, Ł., Yde, J. C.,
460 Takeuchi, N. & Zawierucha, K. (2022). Cryoconite – From minerals and organic
461 matter to bioengineered sediments on glacier's surfaces. *Science of the Total*
462 *Environment*, 807, 150874. <https://doi.org/10.1016/j.scitotenv.2021.150874>

463 Segawa, T., Takeuchi, N., Mori, H., Rathnayake, M. L. D., Li, Z., Akiyoshi, A., Satoh, H. &
464 Ishii, S. (2020). Redox stratification within cryoconite granules influences the nitrogen
465 cycle on glaciers. *FEMS Microbiology Ecology*, 96, fiae199.
466 <https://doi.org/10.1093/femsec/fiae199>

467 Sohm, J. A., Edwards, B. R., Wilson, B. G. & Webb, E. A. (2011). Constitutive extracellular
468 polysaccharide (EPS) production by specific isolates of *Crocospaera watsonii*.
469 *Frontiers in Microbiology*, 2, 229. <https://doi.org/10.3389/fmicb.2011.00229>

470 Stanojković, A., Skoupý, S., Hašler, P., Pouličková, A., Dvořák, P. (2022). Geography and
471 climate drive the distribution and diversification of the cosmopolitan cyanobacterium
472 *Microcoleus* (Oscillatoriales, Cyanobacteria). *The European Journal of Phycology*,
473 57(4), 396–405. <https://doi.org/10.1080/09670262.2021.2007420>

474 Strunecký, O., Elster, J. & Komárek, J. (2010). Phylogenetic relationships between
475 geographically separate *Phormidium* cyanobacteria: is there a link between north and

476 south polar regions? *Polar Biology*, 33, 1419–1428. <https://doi.org/10.1007/s00300->
477 010-0834-8

478 Strunecký, O., Elster, J. & Komárek, J. (2011). Taxonomic revision of the freshwater
479 cyanobacterium „*Phormidium*“ *murrayi* = *Wilmottia murrayi*. *Fottea*, 11, 57–71.
480 <https://doi.org/10.5507/fot.2011.007>

481 Strunecký, O., Komárek, J., Johansen, J., Lukešová, A., Elster, J. (2013). Molecular and
482 morphological criteria for revision of the genus *Microcoleus* (Oscillatoriales,
483 Cyanobacteria). *Journal of Phycology*, 49, 1167–1180.
484 <https://doi.org/10.1111/jpy.12128>

485 Takeuchi, N., Kohshima, S. & Seko, K. (2001). Structure, formation, and darkening process
486 of albedo-reducing material (cryoconite) on a Himalayan Glacier: a granular algal mat
487 growing on the glacier. *Arctic, Antarctic, and Alpine Research*, 33, 115–122.
488 <https://doi.org/10.1080/15230430.2001.12003413>

489 Takeuchi, N., Nishiyama, H. & Li, Z. (2010). Structure and formation process of cryoconite
490 granules on Ürümqi glacier No. 1, Tien Shan, China. *Annals of Glaciology*, 51(56), 9–
491 14. <https://doi.org/10.3189/172756411795932010>

492 Teneva, I., Belkinova, D., Paunova-Krasteva, T., Bardarov, K., Moten, D., Mladenov, R., &
493 Dzhambazov, B. (2023). Polyphasic characterisation of *Microcoleus autumnalis*
494 (Gomont, 1892) Strunecky, Komárek & J.R.Johansen, 2013 (Oscillatoriales,
495 Cyanobacteria) using a metabolomic approach as a complementary tool. *Biodivers.*
496 *Data Journal*, 11, e100525. <https://doi.org/10.3897/BDJ.11.e100525>

497 Uetake, J., Tanaka, S., Segawa, T., Takeuchi, N., Nagatsuka, N., Motoyama, H. & Aoki, T.
498 (2016). Microbial community variation in cryoconite granules on Qaanaaq Glacier,
499 NW Greenland. *FEMS Microbiology Ecology*, 92, fiw127.
500 <https://doi.org/10.1093/femsec/fiw127>

- 501 Vicente-García, V., Ríos-Leal, E., Calderón-Domínguez, G., Cañizares-Villanueva, R. O. &
502 Olvera-Ramírez, R. (2004). Detection, isolation, and characterization of
503 exopolysaccharide produced by a strain of *Phormidium* 94a isolated from an arid zone
504 of Mexico. *Biotechnology & Bioengineering*, 85, 306–310.
505 <https://doi.org/10.1002/bit.10912>
- 506 Wingender, J., Neu, TR., Flemming, H-C. (1999). What are bacterial extracellular polymeric
507 substances? In: Wingender DJ, Neu DTR, Flemming PDH-C (Eds.) *Microbial*
508 *Extracellular Polymeric Substances*. Springer, Berlin Heidelberg, pp. 1–19
- 509 Zawierucha, K., Baccolo, G., Di Mauro, B., Nawrot, A., Szczuciński, W. & Kalińska, E. (2019).
510 Micromorphological features of mineral matter from cryoconite holes on Arctic
511 (Svalbard) and alpine (the Alps, the Caucasus) glaciers. *Polar Science*, 22, 100482.
512 <https://doi.org/10.1016/j.polar.2019.100482>
- 513 Zawierucha, K., Buda, J., Pietryka, M., Richter, D., Łokas, E., Lehmann-Konera, S.,
514 Makowska, N. & Bogdziewicz, M. (2018). Snapshot of micro-animals and associated
515 biotic and abiotic environmental variables on the edge of the south-West Greenland ice
516 sheet. *Limnology*, 19, 141–150. <https://doi.org/10.1007/s10201-017-0528-9>
- 517 Žárský, J., Stibal, M., Hodson, A., Sattler, B., Schostag, M., Hansen, L., Jacobsen, C. &
518 Psenner, R. (2013). Large cryoconite aggregates on a Svalbard glacier support a
519 diverse microbial community including ammonia-oxidizing archaea. *Environmental*
520 *Research Letters*, 8, 035044. <https://doi.org/10.1088/1748-9326/8/3/035044>

521

522

523 **Figures and captions.**

524

525 Figure 1. The experimental design. Inocula of each strain (10 filaments per single inoculum)
526 were transferred into the wells of 24-well plates containing either 1 mL of distilled water
527 alone (control treatment) or different types of mineral particles with 1 mL of distilled
528 water: 1) cryoconite from each sampled glacier, 2) quartz powder. Greenlandic strains
529 were additionally incubated with 3) 1 mL of distilled water and ground up rocks.
530 Scheme created with BioRender.com

531 Figure 2. Cyanobacteria strains used in the experiment: A) *Phormidesmis priestleyi* strain 101
532 (Storglaciären Glacier, Sweden), B) *Phormidesmis priestleyi* strain 102 (Dark Zone,
533 South West Greenland), C) *Phormidesmis priestleyi* strain 103 (South West Greenland,
534 Russel Glacier), D) *Microcoleus autumnalis* strain 104 (Longyearbreen, Spitsbergen,
535 Svalbard). Photos represent specimens of strains fixed with Lugol (left panel) or stained
536 with Alcian blue to reveal EPS. EPS is visible as blue layers surrounding trichomes or
537 empty sheaths. Scale bar on each photo is 10 μm .

538 Figure 3. Probability of granules and mat formation between treatments. The estimates are
539 presented by horizontal lines on a linear scale, while the 95% confidence interval is
540 represented by the grey band. The model outputs, presented in tables, illustrate the
541 estimates on a response scale.

542 Figure 4. Time laps of the treatment: quartz with cyanobacteria, strain 102 (*Ph. priestleyi*,
543 Dark Zone, South West Greenland). The pictures were taken weekly for twelve weeks.

544 Figure 5. View of artificial cryoconite granules and filaments of *Ph. Priestleyi*. A) mixed
545 strains 102 and 103 + rocks. The arrows indicates cyanobacteria filaments while
546 asterisk the cemented granule. B) strain 103 + rocks. Dotted line divides the granule
547 into two layers – surface covered by filaments and cemented part (most likely anoxic).

548 Figure 6. Granules (biogenic structures) in SEM. A) strain 104 (*M. autumnalis*,
549 Longyearbreen, Spitsbergen, Svalbard) + cryoconite (sterilised in 550°C to remove

550 organic matter), view of the formed granule; B) strain 102 (*Ph. priestleyi*, Dark Zone,
551 South West Greenland), view of the mat of glued filaments. C) strain 102 (*Ph.*
552 *priestleyi*, Dark Zone, South West Greenland; strain 103, *Ph. priestleyi* South West
553 Greenland, Russel Glacier) + quartz, view of the granule with *Phormidesmis*
554 filaments. Meaning of the symbols: asterisk – solid and cemented part of the granule,
555 arrowheads – cyanobacterial filaments. All scale bars are in μm .

556 Appendix 1: Molecular methods: 1. Extraction of cyanobacterial DNA, 2. PCR amplification
557 and purification of a product, 3. Molecular identification and phylogeny.

558 Appendix 2: The R script and the data are available in supporting information.

559 Appendix 3: Blast search of the most similar sequences.

560 Appendix 4: Mats and other artificial granules formed during incubation.

561 Figure S1: Maximum likelihood phylogenetic tree of Cyanobacteria, using Tamura 3-parameter
562 algorithm and 1000 bootstrap resampling. The values next to the nodes represent the bootstrap
563 support.

564

565

566

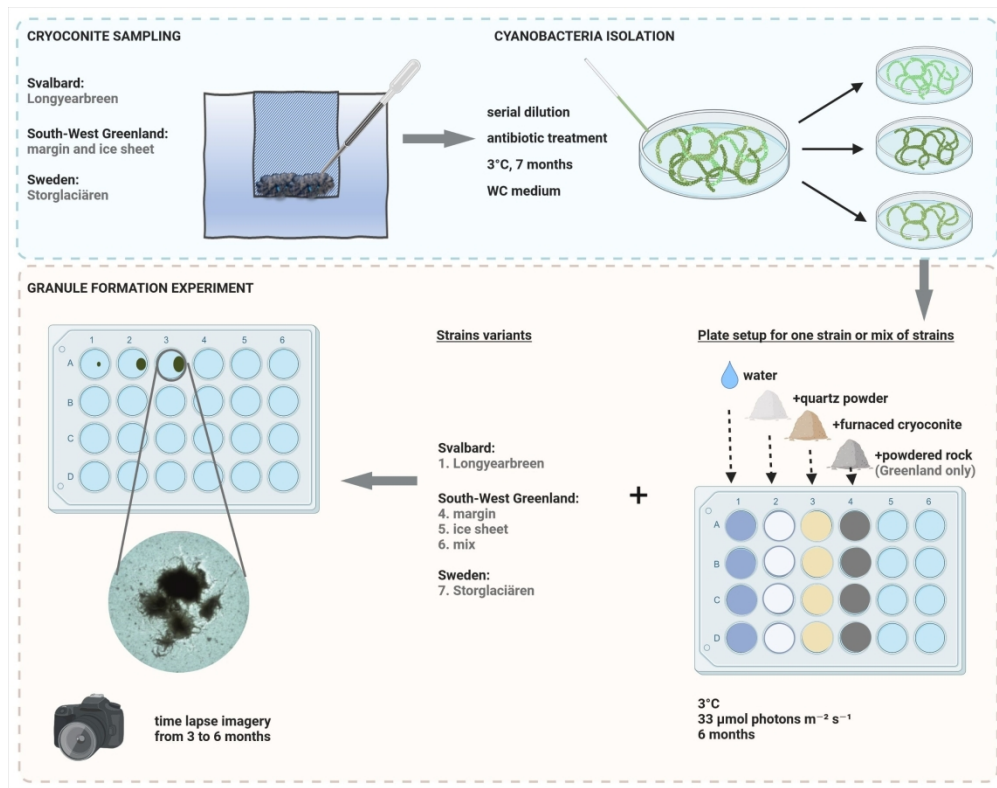
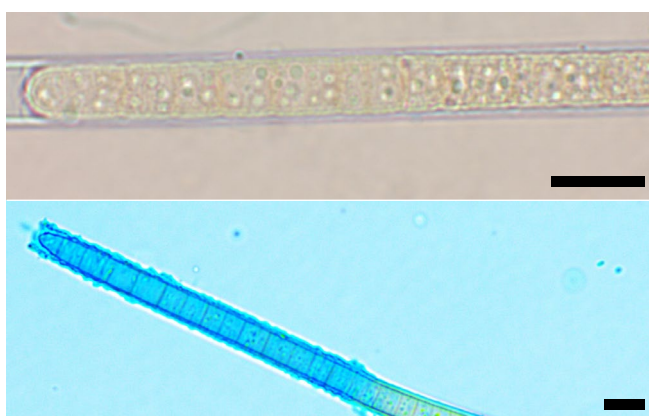
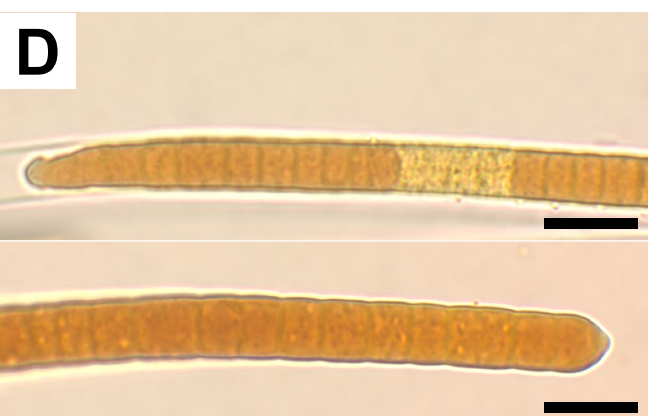
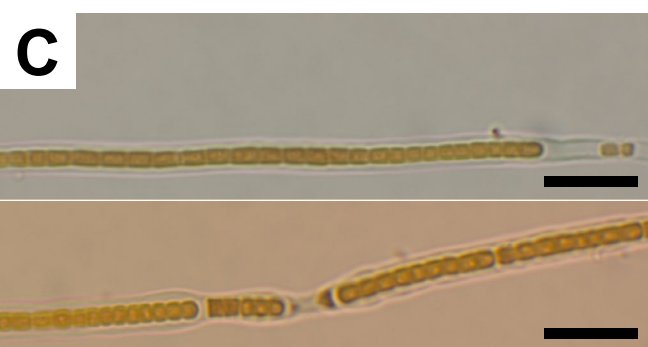
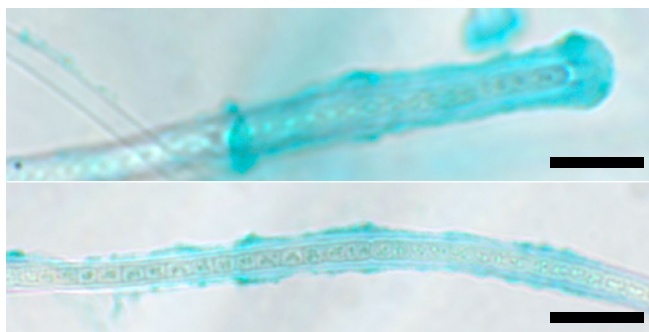
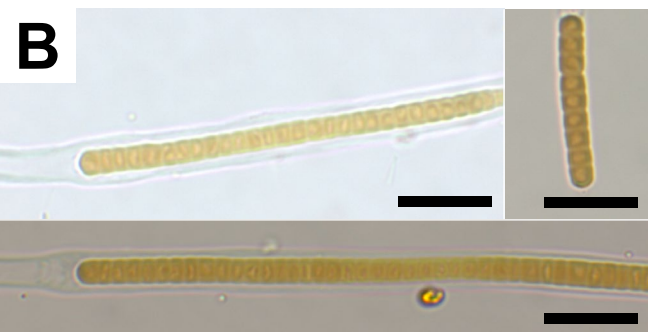
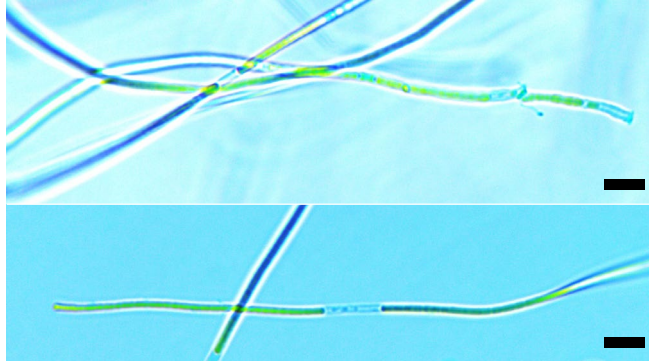


Figure 1. The experimental design. Inocula of each strain (10 filaments per single inoculum) were transferred into the wells of 24-well plates containing either 1 mL of distilled water alone (Control treatment) or different types of mineral particles with 1 mL of distilled water: 1) cryoconite from each sampled glacier, 2) quartz powder. Greenlandic strains were additionally incubated with 3) 1 mL of distilled water and ground up rocks. Scheme created with BioRender.com

Figure 2. Cyanobacteria strains used in the experiment: (a) *Phormidesmis priestleyi* strain 101 (Storglaciären Glacier, Sweden), (b) *Phormidesmis priestleyi* strain 102 (Dark Zone, South West Greenland), (c) *Phormidesmis priestleyi* strain 103 (South West Greenland, Russel Glacier), (d) *Microcoleus autumnalis* strain 104 (Longyearbreen, Spitsbergen, Svalbard). Photos represent specimens of strains fixed with Lugol (left panel) or stained with Alcian blue to reveal EPS. EPS is visible as blue layers surrounding trichomes or empty sheaths. Scale bar on each photo is 10 μm .



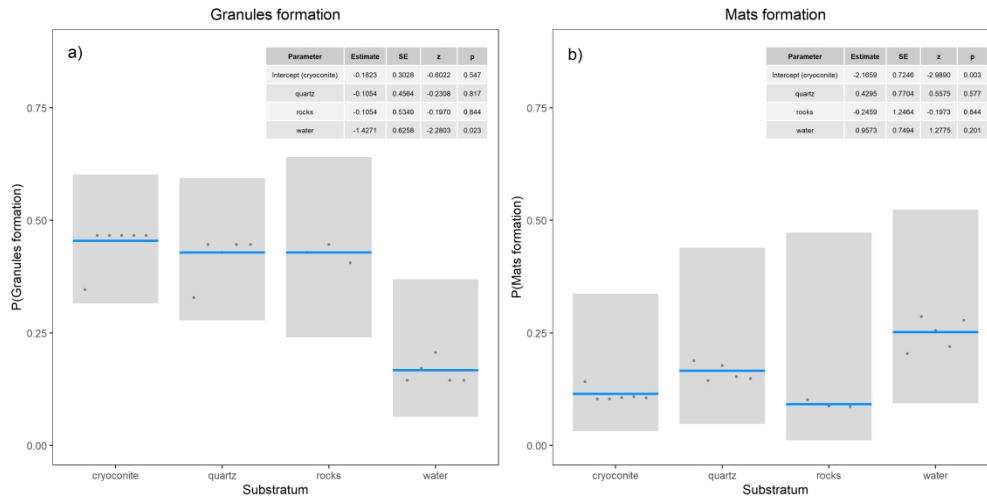


Figure 3. Probability of mat and granule formation between treatments. The estimates are presented by horizontal lines on a response scale, while the 95% confidence interval is represented by the gray band. The model outputs, presented in tables, illustrate the estimates on a linear scale.

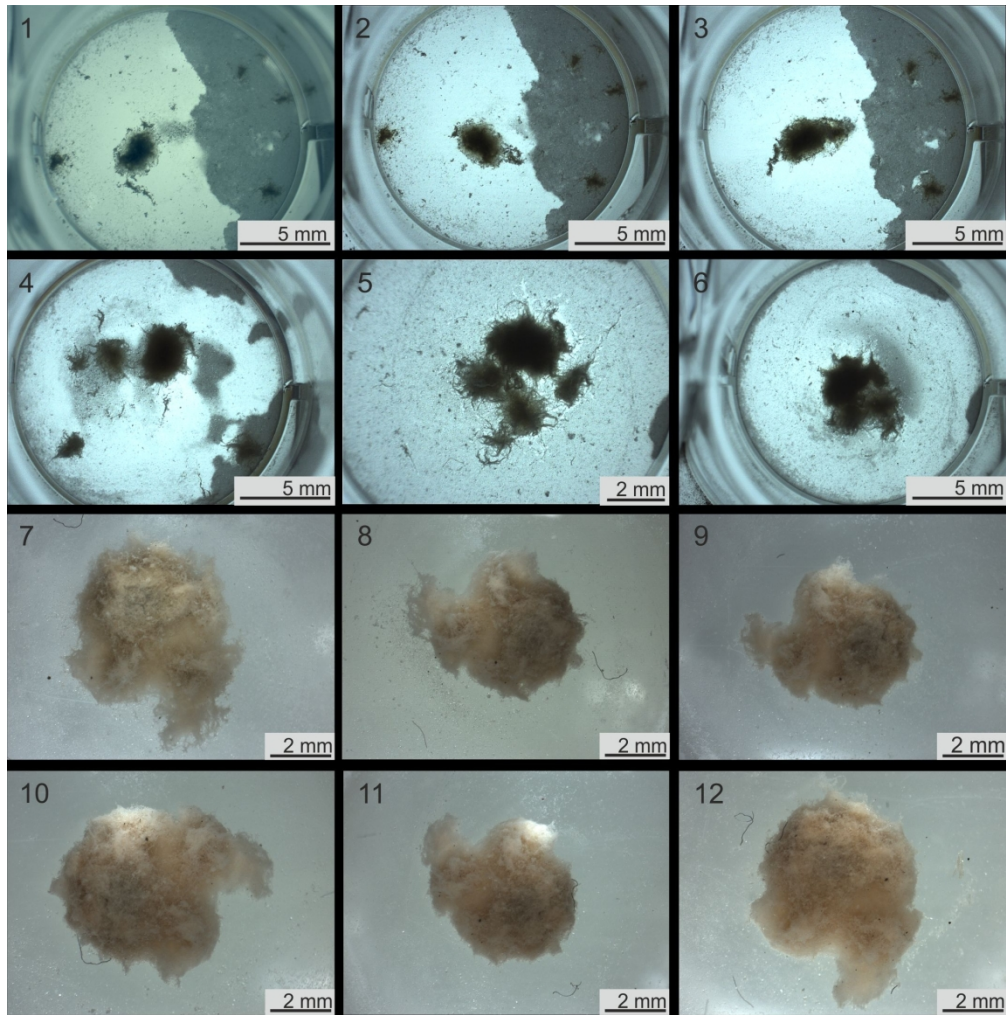


Figure 4. Time lapse of the treatment: quartz with cyanobacteria, strain 102 (*Ph. priestleyi*, Dark Zone, Southwest Greenland). The pictures were taken weekly for 12 weeks.

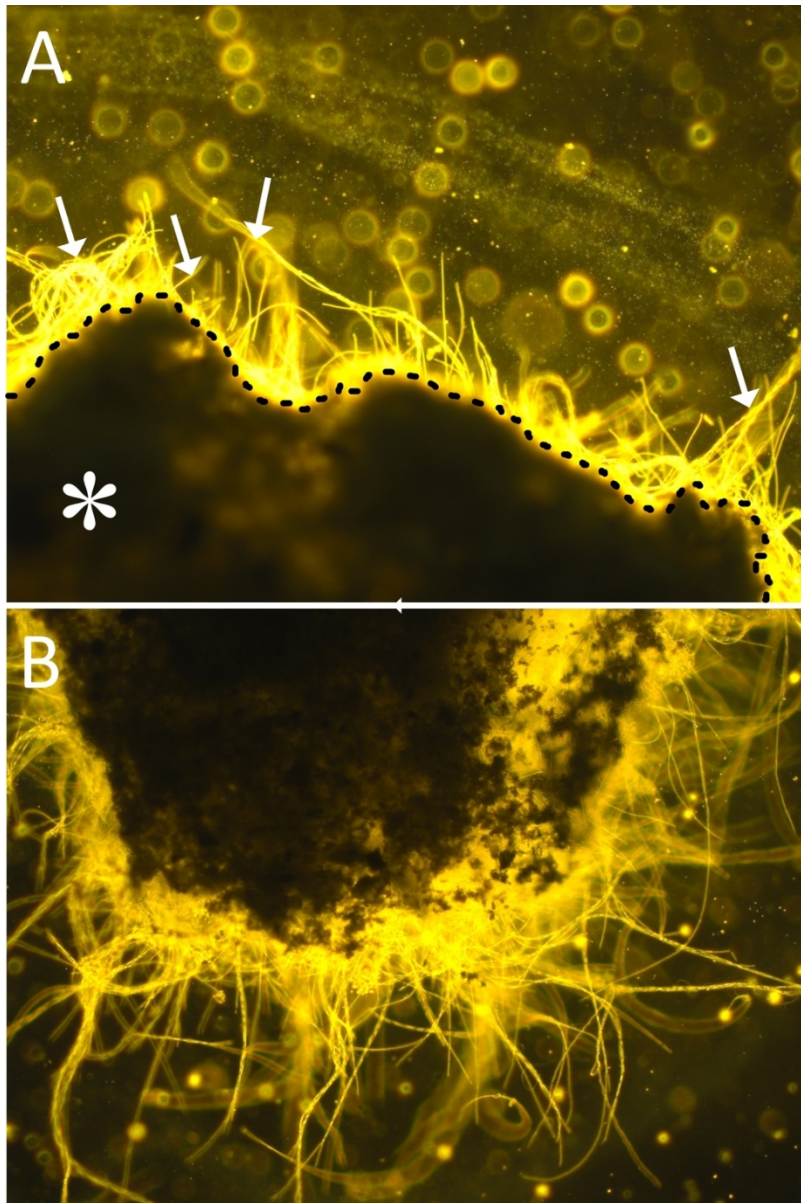


Figure 5. View of artificial cryoconite granules and filaments of *Phormidesmis priestleyi*. (a) Mixed strains 102 and 103+rocks. The arrows indicate cyanobacteria filaments while the asterisk indicates the cemented granule. (b) Strain 103 + rocks. The dotted line in (a) divides the granule into two layers—surface covered by filaments and cemented part (most likely anoxic).

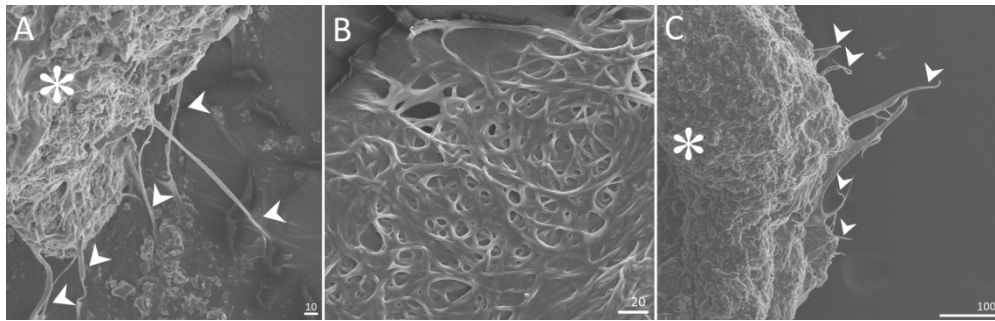


Figure 6. Granules (biogenic structures) in SEM. (a) strain 104 (*Microcoleus autumnalis*, Longyearbreen, Spitsbergen, Svalbard) + cryoconite (sterilized in 550°C to remove organic matter); view of the formed granule; (b) strain 102 (*Phormidesmis priestleyi*, Dark Zone, South West Greenland); view of the mat of glued filaments. (c) strain 102 (*Ph. priestleyi*, Dark Zone, Southwest Greenland; strain 103, *Ph. priestleyi* South West Greenland, Russel Glacier) + quartz; view of the granule with *Phormidesmis* filaments. Meaning of the symbols: asterisk—solid and cemented part of the granule; arrowheads—cyanobacterial filaments. All scale bars are in μm .